Journal of Engineering and Sustainable Development
Vol. 29, No. 05, *August* 2025
https://jeasd.uomustansiriyah.edu.iq/index.php/jeasd
ISSN 2520-0917
Research Article
https://doi.org/10.31272/jeasd.2516

Studying the Physical and Chemical Properties of Polymethyl Methacrylate / Hydroxyapatite Composite for Bone Tissue Engineering

Reman F. Madlol*, Iman J. Abed, Sabah M. Thahab

Materials Engineering Department, Faculty of Engineering, University of Kufa, Najaf, Iraq

*Email: remanf.albaydani@student.uokufa.edu.iq

Article Info

Received	**20/03/2024**
Revised	**09/04/2025**
Accepted	**01/06/2025**

Abstract

The influence of particle aggregation in polymer composite materials is generally affected by polymer-based properties. This study synthesizes polymethyl methacrylate polymers in three concentrations to evaluate their rheological properties at 25 °C. The viscosity and pH of Polymethyl methacrylate PMMA pure and composite polymer solutions are tested. In pure PAMM/acetone, pH increased from 5.3 to 5.4 and then decreased to 4.8 as PMMA increased. PMMA viscosity rises from 17.5 to 32.2 cp, and thermal conductivity falls from 0.301 to 0.205 W/m.K. Hydroxyapatite nano and micro particles with weight ratios of 0.125, 0.25, and 0.5 wt.% are added to PMMA polymer for experiments. Increased micro hydroxyapatite in PMMA raises acidity-base values from 6.91 to 7.15. The acidity drops from 7.12 to 7.00 with nano-hydroxyapatite. The viscosity of the PMMA/HAP composite increases from 17.3 to 18.1 cp for micro-particle size and from 18.1 to 19.1 cp for nanoparticle size as HAP weight ratios increase. With increased micro and nano HAP particle size in polymer composites, thermal conductivity increases from 0.155 to 0.225 W/m · K and from 0.163 to 0.183 W/m·K.

Keywords: Hydroxyapatite; Methyl methacrylate; Microparticles; Nanoparticles

1. Introduction

Polymethyl methacrylate (PMMA) is a colorless polymer with superior light transmission and corrosion resistance [1]. However, PMMA frequently needs more mechanical and thermal stability for high-tech applications. Various nano materials, such as hydroxyapatite (HAP), have been employed as nano fillers to enhance this polymer's functionality [2]. Many biomedical applications use HAP because of its good osteoconductive, biocompatibility, and bioactivity [3]. A brittle material, limited bone formation, and poor mechanical integrity are the limitations of HAP [4]. PMMA is an acrylic material widely used in the medical industry because of its high tensile and flexural modulus. When *PMMA* and *HAP* are combined, a composite material with improved qualities is produced. For instance, PMMA significantly improved density, tensile strength, and flexural modulus [5]. Hydroxyapatite is the main inorganic component of natural bone [6]. Bone is the most significant connective tissue in the human body. He always gets better at supporting weight and healing from injuries. Most bone tissue comprises collagen, hydroxyapatite, fibers, and cells [7].

Polymethyl methacrylate (PMMA) has been extensively employed in biomedical applications, especially in dentistry and orthopedic surgery, owing to its superior transparency, chemical resistance, and considerable mechanical performance [1]. Nonetheless, the intrinsic brittleness and restricted thermal stability of PMMA limit its prolonged clinical use, prompting investigations into composite modifications [5]. Hydroxyapatite (HAP), the primary inorganic constituent of natural bone, has been thoroughly investigated for bone tissue engineering due to its osteoconductive, bioactive, and chemical resemblance to bone mineral [3], [6]. Despite these benefits, pure HAP exhibits brittleness and insufficient toughness, restricting its application in load-bearing contexts [4]. Thus, the integration of HAP with polymers like PMMA provides a means to attain mechanical reinforcement alongside biological compatibility [7].

Recent studies indicate that the integration of HAP into PMMA enhances density, tensile strength, and flexural modulus [5]. Nanostructured HAP exhibits superior dispersion, increased

surface reactivity, and improved bonding with the polymer matrix relative to micro-sized fillers, leading to composites with enhanced mechanical and thermal properties [8],[9]. Challenges persist, including nanoparticle agglomeration and diminished thermal stability at elevated loadings [10].

Numerous reviews have emphasized the potential applications of PMMA/HAP composites in biomedical fields, specifically for dental restorations, bone cements, and implant coatings [1], [3], [11]. Díez-Pascual [5] indicated that PMMA-based nanocomposites exhibit significant potential in odontology, attributed to their enhanced mechanical strength and antimicrobial properties. Awasthi et al. [3] highlighted the significance of HAP coatings for improving the osseointegration of implants. Recent studies have investigated functionalized and porous HAP scaffolds, which may further enhance tissue regeneration [9]. Literature suggests that PMMA/HAP composites effectively address the structural demands of orthopedic materials while meeting the biological requirements for bone regeneration. Optimizing filler concentration, particle size, and dispersion is a critical focus of ongoing research aimed at achieving a balance among mechanical, thermal, and biological properties.

In this research, the preparation and investigation of PMMA/ HAP polymeric solutions as a composite will be carried out and studied. The physical and chemical properties of PMMA/HAP composites will be evaluated and analyzed.

This research aims to synthesize and assess PMMA/HAP composites incorporating both micro- and nano-sized hydroxyapatite particles, to examine the effects of particle size and weight ratios on their physicochemical properties, such as pH, viscosity, UV-visible spectra, and thermal conductivity. The originality of this study resides in the comparative evaluation of micro- and nano-HAP fillers inside a PMMA matrix, highlighting property changes beyond mechanical performance, which are inadequately addressed in current research. The primary contribution of this study is the elucidation of the distinct effects of filler size and concentration on the acidity, viscosity, and thermal properties of PMMA/HAP composites, thereby offering significant insights for the optimization of polymer–ceramic systems in bone tissue engineering applications.

2. Materials and Methods

Micro-sized hydroxyapatite powder within the range of (37-50) μm was used. Its physical properties include the powder density between (2.96 and 3.16) g/cm^3 and an elastic modulus between (70 and 80) GPa, which is purchased from Sunkoo Ltd., South Korea. Also, the nano-sized hydroxyapatite (NHAP) powder of average particle size (30-60 nm) was used. Its physical properties include the following: Elastic modulus varies from (35 to 120) GPa, and powder density between (3.156 to 3.22) g/cm3. These powders were purchased from Alfa Metal Materials Co., Ltd., CHINA. PMMA powder was used, which has the following properties: molecular weight of 15000 g/mol, colorless liquid with 212.9 °F boiling point, purchased from Sigma Aldrich-UK. Acetone with a purity of 99.9% and distilled water (DW) were used as solvents.

2.1. Preparation of Polymer PMMA

Three weights of PMMA polymer (0.3, 0.5, and 0.7 g were taken out and dissolved in 50 ml of pure acetone, namely as C1, C2, and C3, respectively. Followed by mixing solutions using a magnetic stirrer and an ultrasonic instrument. The pH, UV-visible, viscosity, and thermal conductivity measurements were performed for each sample.

2.2. Preparation of PMMA / HAP Composites

To calculate the weight ratio of HAP as filler particles in PMMA solution, the following (1) was used [12]:

$$Vf = \frac{\frac{w_m}{p_m}}{\frac{w_m}{p_m}+\frac{w_p}{p_p}} \quad (1)$$

Where:

Vf =volume fraction of filler in PMMA polymer matrix.

w_m = weight of the matrix.

p_m = density of the matrix.

w_p the weight of particles.

p_p = density of the particles.

Two different *HAP* particle size types were used in this study: nano and micro powder sizes. The PMMA/HAP composites were prepared by adding NHAP (0.125, 0.25, and 0.5 wt%) to (0.7 g / 50 ml) PMMA/acetone solutions receptively. The *pH, UV*-visible, viscosity, and thermal conductivity properties were measured and examined for every composite sample type, as illustrated in Table 2.

Table 1. Illustrate the details of the preparation of PMMA/NHAP.

Polymer solution (g/ml)	The volume fraction of HAP (wt%)	Weight of HAP (g)
C3	0.125	0.062
C3	0.25	0.125
C3	0.5	0.25

2.3 Characterization of PMMA/HAP/ Acetone Composite

UV-Visible spectroscopy of absorbance measurements was carried out using a *PG10* spectrophotometer, CHINA. The thermal conductivities of the PMMA/HAP polymer composite samples were tested using the KD2 Pro thermal properties analyzer (Decagon Devices, Inc., USA). The FTIR spectroscopy is a systematic technique. A rotational viscometer was used. Aed to measure the viscosity characteristics of the composite polymer solutions according to D7945.

Table 2. Illustrate the details of the preparation of PMMA/MHAP.

Polymer solution (g/ml)	The volume fraction of HAP (wt %)	Weight of HAP (g)
C3	0.125	0.062
C3	0.25	0.125
C3	0.5	0.25

3. Results and Discussion

3.1. Pure PMMA/Acetone Polymer Solution

3.1.1. PH study

Fig. 1 shows *PH* measurement values as a function of weight PMMA concentrations. It was observed that the acidity value increases from 5.3 to 5.4 and then decreases to 4.8 with the increasing PMMA weight concentration. This could be attributed to the hydrolysis reactions occurring at these concentrations. Additionally, the release of carboxylic acids from the polymer could lead to increased acidity. However, the acidity decreases at high concentrations of *PMMA* due to the reduced intensity of hydrolase reactions that occur at this concentration. This causes the least amount of carboxylic acids to be released from the polymer, which leads to a decrease in acidity, as shown in Fig. 1 [13].

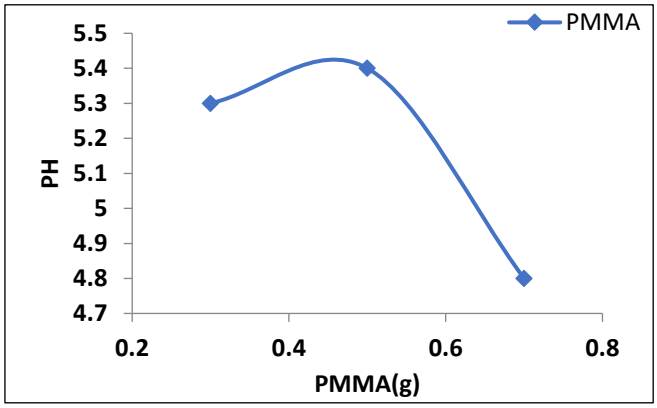

Figure 1. PH measurements values as a function of weight PMMA concentrations.

3.1.2. UV-visible study of pure PMMA polymer

UV-visible spectrum was used to investigate the optical properties of PMMA/Acetone. Fig. 2 shows the UV-visible spectrum of different PMMA weight concentrations. The *PMMA* spectrum peak wavelength is located at 205nm for the lower concentration. However, a red shift was observed at higher *PMMA* concentrations of C2 and C3, respectively [14].

3.1.3. Viscosity characterization of pure polymer PMMA/acetone

Fig.3 reveals that with an increase in the *PMMA*/acetone concentrations, the viscosity also increases from 17.5 to 32.2 cp due to the high crosslinking of polymer chains. The number of reactive imides increases as the PMMA weight concentration rises, further enhancing intermolecular strength [15].

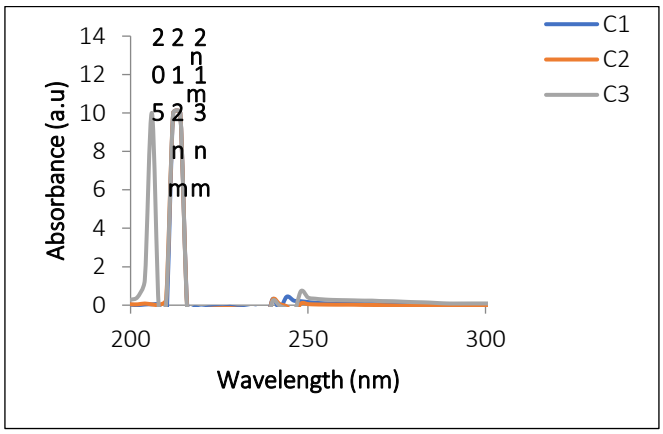

Figure 2. UV-Visible spectra as a function of PMMA weight concentrations.

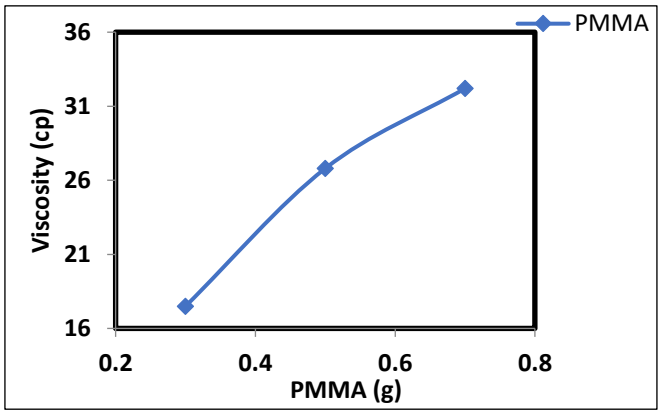

Figure 3. Viscosity measurement values as a function of PMMA weight concentrations.

3.1.4. Thermal conductivity of pure PMMA polymer

As the weight concentration of PMMA polymer increases, it will lead to a decrease in thermal conductivity from 0.301 to 0.205 W/m. K, as shown in Fig. 4. This could be a script for the expansion of the polymer chains and the appearance of larger gaps when the PMMA polymer concentration increases, which will lead to it acting as a better thermal insulator at high concentrations [16].

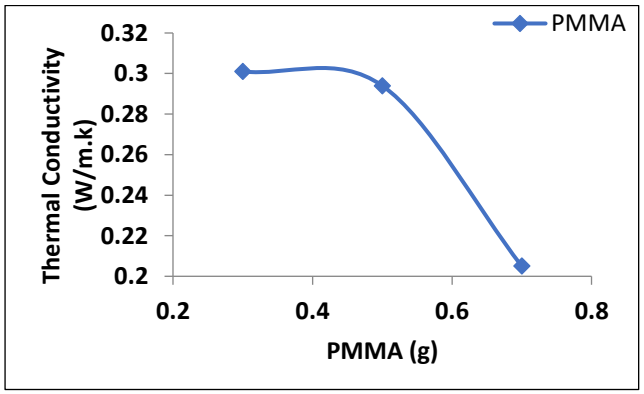

Figure 4. Thermal conductivity measurement values as a function of PMMA weight concentrations.

3.2. Characterization of HAP Powders

3.2.1. Fourier transform infrared spectroscopy (FTIR) of HAP powders

3.2.1.1. Micro HAP powder

The *FTIR* peaks with several bands that belong to MHAP powder are revealed in Fig.5. The phosphate (PO_4)-3 (bending mode) vibrational modes' reflections are responsible for the weak peak at 603 cm-1. The carbonate (CO_3) -1group of *HAP* is shown by the peak at 837 cm-1 in the spectrum (bending mode). The presence of apatite structure is confirmed by the 1036 cm-1 bands, which are associated with the symmetric stretching vibrational modes of phosphate (PO4)-3. Also, the existence of the carbonate (CO_3)-1group (symmetric stretching) is shown by the peak at 1401 cm-1. The band proves the water adsorption at 1642 cm-1, which corresponds to the hydroxyl group's (OH) bending mode vibrations [17]. The two sharp 2853 cm−1 and 2923 cm−1 absorption bands correspond to the symmetric and asymmetric C-H stretching vibrations of molecules [18], [19]. Finally, the 3400 cm-1 bands are attributed to vibrations of the hydroxyl group (OH) (stretching) [20].

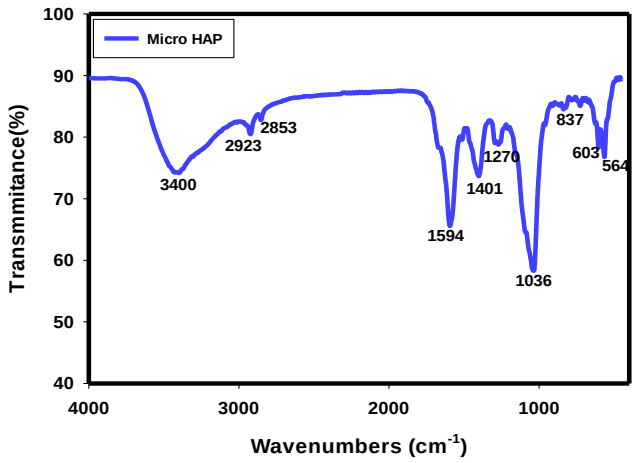

Figure 5. FTIR spectrum of MHAP powder.

3.2.1.2. FTIR of nano HAP powder

FTIR results for the *NHAP* powder are shown in Fig. 6. The peak located at 471cm.$_1$ is related to vibrational (ν_2). The characteristic absorption bands for the anti-symmetric (ν_4) of the phosphate groups PO_4^{-3} at 564 cm^{-1} and 602 cm^{-1} are a feature of crystalline HAP [8]. The band presented at 962 cm^{-1} corresponds to the symmetrical stretching (ν_1) P–O, and peaks at 1033 and 1091 cm^{-1} originated from the asymmetric (ν_3) P–O stretching mode. CO_3^{-2} bands were identified at peaks 1418 cm^{-1}, asymmetric C-O stretching. Whereas, the peaks at (875 cm^{-1} and 1452 cm^{-1}) were exhibited due to absorption bands to (ν_2) O-C-O bending. In addition, bands at 3434 cm^{-1} related to (OH) groups and the peak in 1624 cm^{-1} is for δ(O-H), which proves the presence of water in the HAP lattice.

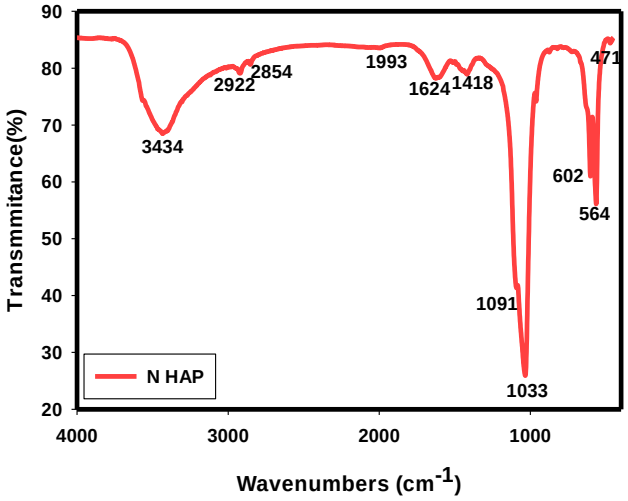

Figure 6. FTIR spectrum of NHAP powder.

3.2.2. UV-visible study of HAP powders

Pure HAP powder exhibits optical peak wavelength absorption in the UV-Visible range of (200–340) nm. Fig.7 reveals the presence of the wavelength peak absorption of nano- and micro-sized HAP powders located at 206 nm and 238 nm, respectively [8].

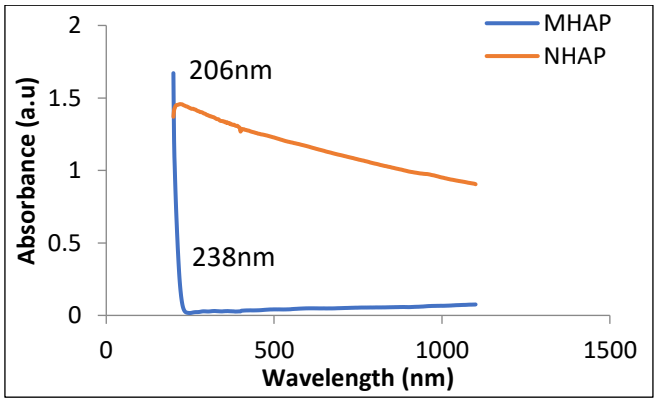

Figure 7. UV-Visible spectra of HAP powder.

3.3. Physical and Chemical Properties Of PMMA/HAP Composite

3.3.1. PH studies of PMMA /HAP composites

Fig. 8 reveals the PH measurements values of PMMA/ HAP polymer composite as a function of HAP powder weight percentage ratio. It can be seen that an increase in acidity values from 6.91 to 7.15 occurs when MHAP powders are added to the PMMA polymer matrix. This could be related to the hydrogen ions contained in MHAP powder, which leads to an increase in the concentration of hydrogen ions in the solution and results in an increase in acidity [9]. In addition, variations in PH values in the range (7.12-7.00) are observed in the PMMA/NHAP composite. This behavior can be attributed to the disbanding of the compounds present. When NHAP particles surround the molecules of polymers, they will prevent those molecules from attaching [11].

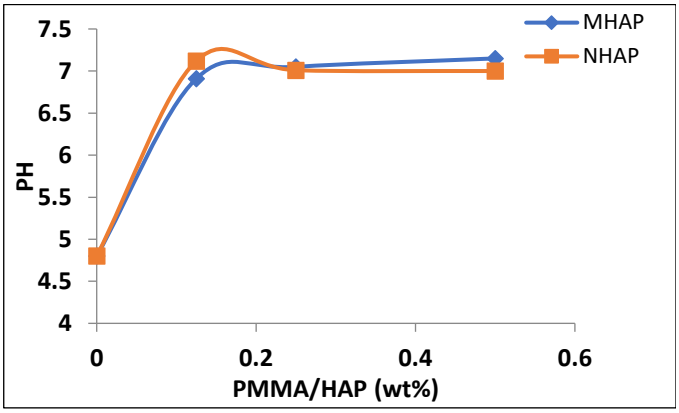

Figure 8. PH relation as a function of PMMA/ HAP (wt%).

3.3.2. UV-visible spectra of PMMA /HAP composites

The UV-visible absorbance spectra of the micro and nanocomposite PMMA/HAP are shown in Fig. 9 and Fig. 10, respectively. It is clear that when the composite concentration of MHAP rises, the dispersion and absorption of light cause this rise in absorption [21]. Also, the PMMA/NHAP absorbance spectra variation could be related to several flaws at the nanoscale, including tiny size, instability, and agglomeration ability.

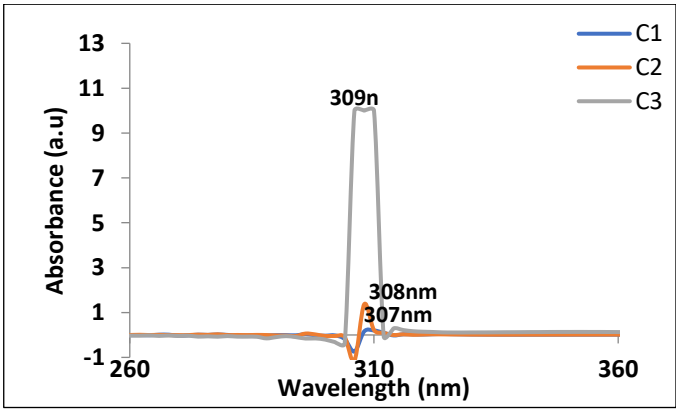

Figure 9. UV-Visible spectra of PMMA/MHAP polymer composite

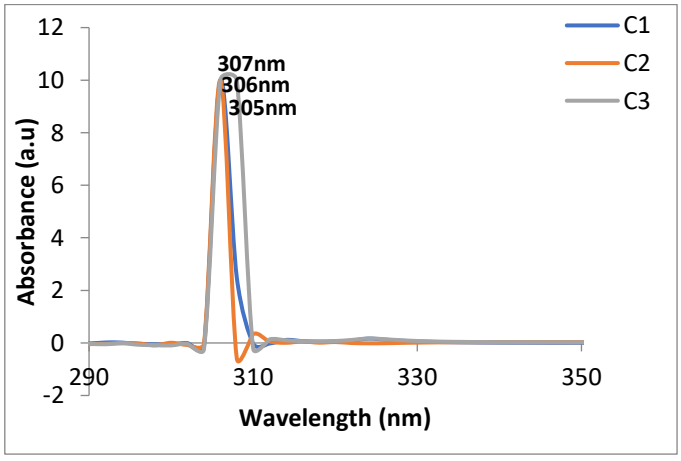

Figure 10. UV-Visible spectra of PMMA/NHAP polymer composite.

3.3.3. Viscosity analysis of PMMA /HAP composites

Fig. 11 reveals the relationship between viscosity measurements and PMMA/HAP polymer composite as a function of HAP powder weight percentage ratios. It can be seen that the viscosity values of PMMA/MHAP change and increase from 17.3 to 18.1 cp as the wt% of MHAP powders increases. Increases from 18.1 to 19.1 cp when adding NHAP powders are also observed. The reason for an increase in viscosity values in both PMMA/HAP micro and nano composites is the increase in crosslinking between the molecular chains.

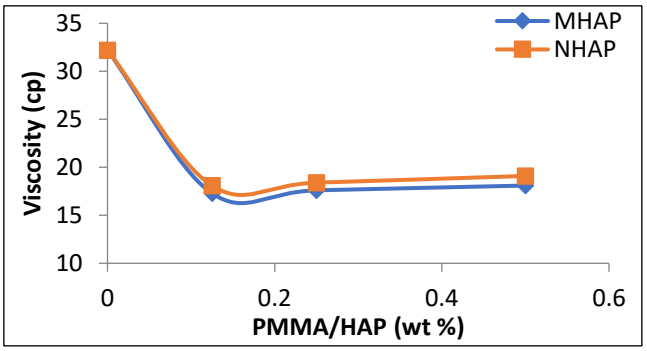

Figure 11. Viscosity variation as a function of PMMA/HAP polymer composite (wt%).

3.3.4. Thermal conductivity characterizations of PMMA /HAP polymer composite

Fig. 12 shows the thermal conductivities of the PMMA/HAP polymer composites. It is observed that the thermal conductivity of PMMA/HAP polymer micro-composites increases from 0.155 to 0.225 W/m.K. At the same time, the thermal conductivity increases from 0.163 to 0.183 W/m · K in PMMA/NHAP polymer nanocomposites, which is less than that observed in the micro composite. This could be attributed to the effect of particle size and shape, which tends to influence and induce different scattering types in different crystal locations. The small size of such particles could also influence and present various defects, and the ability to undergo particle agglomeration. As the volume fraction of the HAP NPs increases, the thermal conductivity increases, which agrees well with the previous research findings [10].

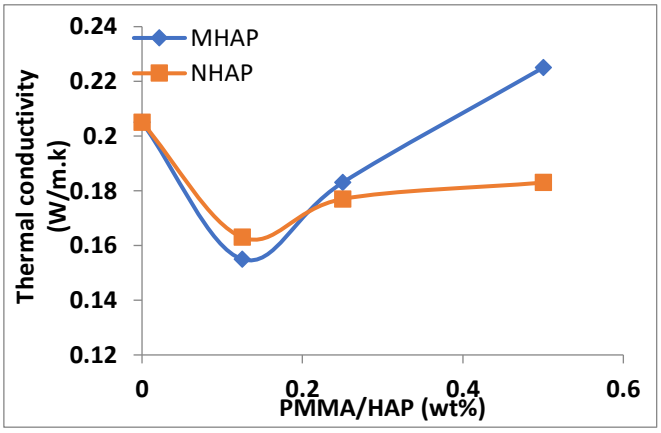

Figure 12. Thermal conductivity variation as a function of PMMA/HAP polymer composite (wt%).

3.3.5. Structural properties of PMMA /HAP composite

Fig.13 (a and b) shows the FESEM images of the PMMA/MHAP at different magnifications. It can be observed that as the van der Waals interactions are present between the particles, the MHAP powder tends to agglomerate. As a result, the sample contains aggregated crystallites with large diameters. The powder particle crystallites are separated by the grain boundary, which would affect the powder's optical characteristics. The distribution of the crystallite size ranges from tens of nanometers to several micrometers.

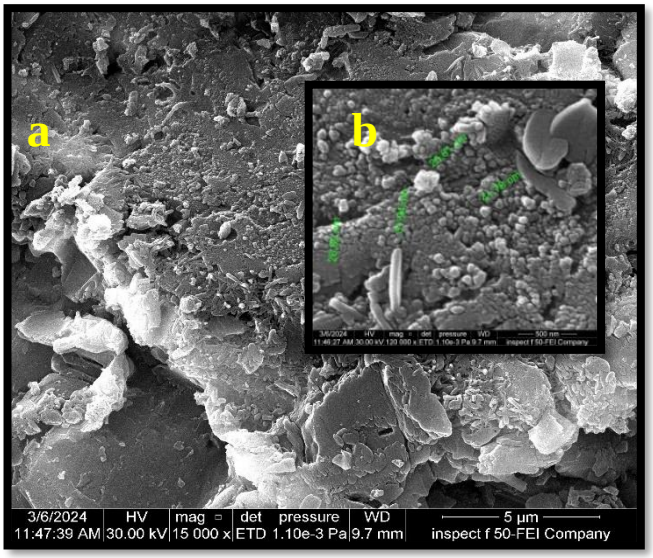

Figure 13. SEM images of PMMA/MHAP composite (a) 5 µm and (inset (b) 500 nm.

Fig. 14 (a and b) shows the FESEM images of the PMMA/NHAP at magnification values of (a) 5 µm and (b) 500 nm, respectively. The surface morphology of the PMMA/NHAP polymer nanocomposite film revealed some aggregates or fragments that were randomly scattered on the upper surface of the PMMA polymer. The obtained results indicated that when the NHAP nano powder is dispersed in the PMMA polymer matrix, some NHAP particles tend to form microscopic aggregates. From the FESEM image, the average particle size of the distributed NHAP nanoparticles in the PMMA composite ranges from 17 to 32 nm. This could be attributed to the effects of heat polymerization associated with continuous sonication mixing, which induces the NHAP particles to be well de-agglomerated and stabilized [22].

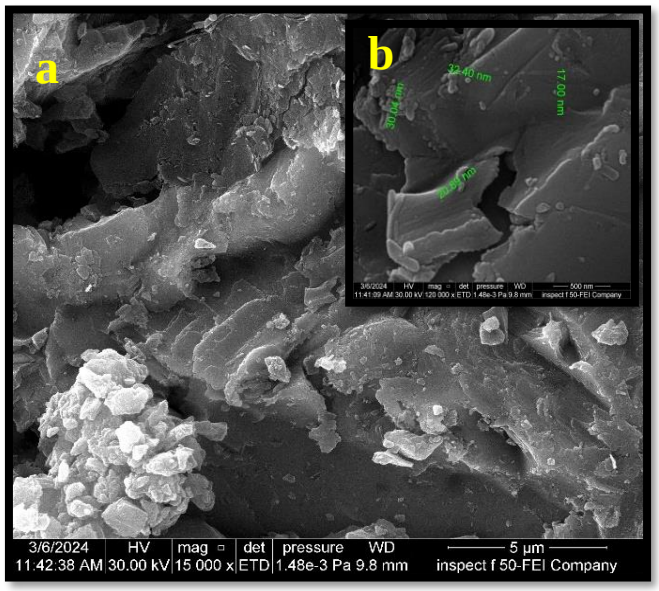

Figure 14. SEM images of PMMA/NHAP composite (a) 5 µm and (inset (b) 500 nm.

4. Conclusions

The hydrolysis reactions at various concentrations of PMMA polymer exhibited a variation in acidity levels. Initially, the acidity increased from 5.3 to 5.4 and subsequently decreased to 4.8 as the weight concentration of PMMA increased. Moreover, the acidity of the PMMA/HAP composite was found to vary based on the size of the incorporated HAP particles. The absorbance spectra demonstrated a positive correlation between the concentration of micro-HAP and the absorbance value, with the absorbance value increasing as the micro-HAP concentration increased. Furthermore, the viscosity values of the pure PMMA polymer increased as the PMMA weight concentration increased. The thermal conductivity values of PMMA/NHAP nanocomposite polymers decreased as the weight percentage ratio of HAP nanoparticles increased. Conversely, the thermal conductivity of PMMA/MHAP micro composite increased with higher weight percentage ratios. This can be attributed to the effects of thermal conductivity and surface scattering of particles on the aggregate properties of filler particles in the polymer matrix.

Acknowledgments

The authors would like to acknowledge the assistance provided by the Nanotechnology and Advanced Materials Research Unit (NAMRU), Faculty of Engineering, University of Kufa, IRAQ.

Abbreviations

PMMA	Poly Methyl methacrylate
HAP	hydroxyapatite
NHAP	nano hydroxyapatite
MHAP	micro hydroxyapatite
FTIR	Fourier transform infrared spectrophotometer
Ps	particle size

Conflict of Interest

No conflicts of interest regarding the publication of this manuscript.

Author Contribution Statement

Reman Fouad: did the experimental work and wrote the manuscript. Iman J. Abed read and edited the manuscript. S.M. Thahab rechecked and corrected the manuscript format and the figures' plotting style.

References

[1] M. S. Zafar, "Prosthodontic applications of polymethyl methacrylate (PMMA): An update," *Polymers*, vol. 12, no. 10, p. 2299, Oct. 2020, doi: https://doi.org/10.3390/polym12102299 .

[2] W.-J. Yang et al., "Fire-retarded nanocomposite aerogels for multifunctional applications: A review," *Compos. Part B Eng.*, vol. 237, p. 109866, May 2022, doi: https://doi.org/10.1016/j.compositesb.2022.109866.

[3] S. Awasthi, S. K. Pandey, E. Arunan, and C. Srivastava, "A review on hydroxyapatite coatings for the biomedical applications: Experimental and theoretical perspectives," *J. Mater. Chem. B*, vol. 9, no. 2, pp. 228–249, 2021, doi: https://doi.org/10.1039/D0TB02407D.

[4] A. Mahanty and D. Shikha, "Changes in the morphology, mechanical strength and biocompatibility of polymer and metal/polymer fabricated hydroxyapatite for orthopaedic implants: A review," *J. Polym. Eng.*, vol. 42, no. 4, pp. 298–322, Feb. 2022, doi: https://doi.org/10.1515/polyeng-2021-0171.

[5] A. M. Díez-Pascual, "PMMA-based nanocomposites for odontology applications: A state-of-the-art," *Int. J. Mol. Sci.*, vol. 23, no. 18, p. 10288, Sep. 2022, doi: https://doi.org/10.3390/ijms231810288.

[6] S. Sathiyavimal et al., "Natural organic and inorganic–hydroxyapatite biopolymer composite for biomedical applications," *Prog. Org. Coat. *, vol. 147, p. 105858, Oct. 2020, doi: https://doi.org/10.1016/j.porgcoat.2020.105858.

[7] M. Mallick, R. P. Are, and A. R. Babu, "An overview of collagen/bioceramic and synthetic collagen for bone tissue engineering," *Materialia*, vol. 22, p. 101391, May 2022, doi: https://doi.org/10.1016/j.mtla.2022.101391.

[8] W. D. Callister, Jr. and D. G. Rethwisch, *Materials Science and Engineering: An Introduction*, 10th ed. Wiley, 2018.

[9] S. K. Singh et al., *Polymeric Micelles: Principles, Perspectives and Practices*. Springer, 2023.

[10] N. R. Barveen et al., "Flexible silver-nanoparticles/PMMA SERS substrate derived from nanotips-equipped chemically patterned ferroelectric crystals for detecting antibiotics on irregular surfaces," *Surf. Interfaces*, vol. 41, p. 103169, Oct. 2023, doi: https://doi.org/10.1016/j.surfin.2023.103169.

[11] N. K. Farhana et al., "Review on the revolution of polymer electrolytes for dye-sensitized solar cells," *Energy Fuels*, vol. 35, no. 23, pp. 19320–19350, Nov. 2021, doi: https://doi.org/10.1021/acs.energyfuels.1c03039.

[12] Z. Xu et al., "Enhanced thermal conductivity and electrically insulating of polymer composites," *J. Mater. Sci.*, vol. 56, no. 6, pp. 4225–4238, Nov. 2020, doi: https://doi.org/10.1007/s10853-020-05530-5 .

[13] M. Greiner et al., "Combined influence of reagent concentrations and agar hydrogel strength on the formation of biomimetic hydrogel–calcite composites," *Cryst. Growth Des. *, vol. 18, no. 3, pp. 1401–1414, Jan. 2018, doi: https://doi.org/10.1021/acs.cgd.7b01324.

[14] A. B. D. Nandiyanto, R. Oktiani, and R. Ragadhita, "How to read and interpret FTIR spectroscope of organic material," *Indones. J. Sci. Technol.*, vol. 4, no. 1, p. 97, Mar. 2019, doi: https://doi.org/10.17509/ijost.v4i1.15806.

[15] N. Chetry, T. Karlo, and T. G. Devi, "Intermolecular interaction study of Ag-amino acid biomolecular complex using vibrational spectroscopic techniques and density functional theory method," *J. Mol. Struct. *, vol. 1266, p. 133410, Oct. 2022, doi: https://doi.org/10.1016/j.molstruc.2022.133410.

[16] T. Theophanides, "Introduction to infrared spectroscopy," in *Infrared Spectroscopy - Materials Science, Engineering and Technology*, InTech, 2012, doi: https://doi.org/10.5772/47117.

[17] A. Sindhya et al., "Synthesis and characterization of nanohydroxyapatite (nHAp) from *Meretrix meretrix* clam shells and its in-vitro studies for biomedical applications," *Vacuum*, vol. 204, p. 111341, Oct. 2022, doi: https://doi.org/10.1016/j.vacuum.2022.111341.

[18] S. Bhat et al., "Functionalized porous hydroxyapatite scaffolds for tissue engineering applications: A focused review," *ACS Biomater. Sci. Eng.*, vol.. 8, no. 10, pp. 4039–4076, Sep. 2021, doi: https://doi.org/10.1021/acsbiomaterials.1c00438 .

[19] S. Singh et al., "Transformation of PMMA from sunlight-blocking to sunlight-activated coupled with DNH photocatalytic platform for oxidative coupling of amines and generation/regeneration of LDC/NADH," *Photochem. Photobiol. *, Dec. 2023, doi: https://doi.org/10.1111/php.13888.

[20] G. Soni et al., "Optical, mechanical and structural properties of PMMA/SiO_2 nanocomposite thin films," *Mater. Res. Express*, vol. 5, no. 1, p. 015302, Jan. 2018, doi: https://doi.org/10.1088/2053-1591/aaa0f7.

[21] Q. Chen et al., "Planar heterojunction perovskite solar cells via vapor-assisted solution process," *J. Am. Chem. Soc.*, vol. 136, no. 2, pp. 622–625, Dec. 2013, doi: https://doi.org/10.1021/ja411509g .

[22] P. D. Shima, J. Philip, and B. Raj, "Influence of aggregation on thermal conductivity in stable and unstable nanofluids," *Appl. Phys. Lett. *, vol. 97, no. 15, Oct. 2010, doi: https://doi.org/10.1063/1.3497280 .